J. Math. Anal. Appl. 347 (2008) 179–187

Contents lists available at ScienceDirect

J. Math. Anal. Appl.

www.elsevier.com/locate/jmaa

Noise perturbed generalized Mandelbrot sets ☆

Wang Xingyuan *, Wang Zhen, Lang Yahui, Zhang Zhenfeng

School of Electronic & Information Engineering, Dalian University of Technology, Dalian 116024, China

ARTICLE INFO

Article history:
Received 3 February 2007
Available online 20 April 2008
Submitted by L. Guo

Keywords:
Noise perturbed
Generalized M-sets
Fractal
Brownian movement

ABSTRACT

Adopting the experimental mathematics method of combining the theory of analytic function of one complex variable with computer aided drawing, in this paper on the structure characteristics and the discontinuity evolution law of the additive noise perturbed generalized Mandelbrot sets (M-sets) was studied. On the influence of stochastic perturbed parameters of the structure of generalized M-sets was analyzed. The physical meaning of the additive noise perturbed generalized M-sets was expounded.

0. Introduction

In recent 20 years, people have lucubrated on the generalized Mandelbrot-sets (M-sets in short) constructed from the complex map $z_{n+1} = z_n^{\alpha} + c$ ($\alpha \in R$) and found there existed orderly structure in it [1,2]. For example, Gujar et al. proposed several assumptions based on the visually structural characteristics of generalized M-sets [3]; Glynn found the symmetrical evolution of generalized M-sets when the phase angle $\theta \in [-\pi, \pi)$ [4]; the authors put forward the embedded topological distribution theorem of the generalized M-sets and discussed the different selections of the principal value range of the phase angle θ and the fission-evolution rule of the generalized M-sets for decimal index number [5]; Sasmor analyzed the fission of generalized M-sets for rational index number when the phase angle $\theta \in [-\pi, \pi)$ [6]; Romera and Pastor et al. researched on the embedded-layer relationship of bud of generalized M-sets in the Misiurewicz points [7,8]; Geum and the authors both studied the structure and distribution of the periodic bud of generalized M-sets and the topological rule of their periodic trajectories [9,10]; Beck and the authors both discussed the physical meaning of generalized M-sets [11,12]. Furthermore, Argyris, Lasota, Kapitaniak, et al. discussed the classification and affection of noise in complex dynamical system [13–15]; Argyris et al. studied the structural characteristic of M-sets containing noise after importing additive noise and multiplicative noise into the complex map $z_{n+1} = z_n^2 + c$ [16–18]. Based on above researches, this paper studied the structural characteristic and fission-evolution law of stochastic perturbed generalized M-sets, analyzed the influence of stochastic perturbed parameters of the structure of generalized M-sets and expatiated on the physical meaning of a type of generalized M-sets.

1. Theory and method

Noise is a type of random variable. It can be divided into additive noise and multiplicative noise according to its appearance style in dynamical equations. In general, the dynamical system for discrete time domain in Euclidean space R^r is denoted as follows:

☆ This research is supported by the Chinese National Natural Science Foundation (No. 60573172), the Doctoral Program Foundation of Institution of Higher Education of China (No. 20070141014).

* Corresponding author.
E-mail address: wangxy@dlut.edu.cn (X. Wang).

0022-247X/$ – see front matter
doi:10.1016/j.jmaa.2008.04.032

$$x_{n+1} = F(x_n, \lambda, n), \tag{1}$$

where $x_n \in R^r$, $\lambda \in R^\nu$, $n \in N$, the function F has an attractor with at least one correlation dimension being not ∞ in Eq. (1). If added additive noise, then Eq. (1) turns into

$$x_{n+1} = F(x_n, \lambda, n, \boldsymbol{w}_n). \tag{2}$$

For dynamical system for discrete time domain, Eq. (2) can be rewrite into

$$x_{n+1} = F(x_n, \lambda, n) + \boldsymbol{w}_n. \tag{3}$$

If added multiplicative noise, then Eq. (1) becomes

$$x_{n+1} = F\big(x_n, \gamma(\lambda, \boldsymbol{w}_n), n\big), \tag{4}$$

where $\boldsymbol{w}_n$ denotes noise vector, γ is a function correlating with alternated variable x, λ is polynomial coefficient needing to be determined.

When construct stochastic perturbed parameters of the dynamics system, we adopt macmcyclic identical deflected stochastic numerical arithmetic, which was brought forward by L'Ecuyer [19], improved using additional Bays–Durham shuffle arithmetic by Press et al. [20], to simulate noise. To great extent, the arithmetic destroys the stochastic numerical ordered dependency, as long as a negative integer initial value is given to be the seed, a random number which has good randomicity in the interval of $(0, 1)$ can be generated, so the noise can simulate the noise realistically. To study the affection of stochastic perturbation to generalized M-sets, we import the noise as a sort of stochastic perturbation into the complex map constructing generalized M-sets. All analyses are summarized as follows.

Import the additive noise in Eq. (3) into the complex map used to construct generalized M–J sets. We can obtain the equation shown as follows

$$z_{n+1} = z_n^\alpha + W + c \quad (\alpha \in R), \tag{5}$$

where $W = m_1 \boldsymbol{w}_n + m_2 \boldsymbol{w}_n i$ $(m_1, m_2 \in R)$ is the dynamic additive noise perturbation, and m_1 and m_2 are the intensity coefficients of the real part of additive perturbation W and imaginary part of noise $\boldsymbol{w}_n$, respectively. Eq. (5) can be turned into two-dimensional discrete map

$$\begin{cases} x_{n+1} = f_1(x_n, y_n, m_1, m_2), \\ y_{n+1} = f_2(x_n, y_n, m_1, m_2). \end{cases} \tag{6}$$

When $m_1 = m_2$, Eq. (6) satisfies Cauchy–Riemann condition [21]

$$\begin{cases} \partial f_1(x, y)/\partial x = \partial f_2(x, y)/\partial y, \\ \partial f_1(x, y)/\partial y = -\partial f_2(x, y)/\partial x. \end{cases} \tag{7}$$

So Eq. (5) is analytic mapping; when $m_1 \neq m_2$, Eq. (6) does not satisfy Eq. (7), so Eq. (5) is non-analytic mapping.

If multiplicative noise in Eq. (4) is imported into complex map constructing generalized M-sets, then

$$z_{n+1} = \gamma(\lambda, k_1, k_2, \boldsymbol{w}_n) z_n^\alpha + c \quad (\alpha \in R), \tag{8}$$

where k_1 and k_2 $(k_1, k_2 \in R)$ denote intensity coefficients of the inlet perturbation $\boldsymbol{w}_n$ that multiplicative perturbation γ is on the x-axis and y-axis of the dynamical system F.

Start to iterate from the critical point of f or g if generalized M-set is to be constructed from the complex mapping $f(z_n) = z_n^\alpha + W + c$ or $g(z_n) = \gamma(\lambda, k_1, k_2, \boldsymbol{w}_n) z_n^\alpha + c$ $(\alpha \in R)$. However when $\alpha > 1$, the critical point of f is 0, so if $z_0 = 0$, then $z_1 = W + c$, $z_2 = (W + c)^\alpha + W + c, \ldots$ can be obtained; the critical point of g is 0, so if $z_0 = 0$, then $z_1 = c$, $z_2 = \gamma(\lambda, k_1, k_2, \boldsymbol{w}_n) c^\alpha + c, \ldots$ can be obtained. When $\alpha < 0$, the critical point of f is ∞, so if $z_0 = \infty$, then $z_1 = W + c$, $z_2 = (W + c)^\alpha + W + c, \ldots$ can be obtained; the critical point of g is ∞, so if select $z_0 = \infty$, then $z_1 = c$, $z_2 = \gamma(\lambda, k_1, k_2, \boldsymbol{w}_n) c^\alpha + c, \ldots$ can be obtained. Therefore, to avoid computer overflow, the iterative initial point of f can be selected as $z_0 = W + c$, and the iterative initial point of g is $z_0 = c$. It is notable that when $\alpha \in [0, 1]$, the genuine generalized M-set cannot be obtained if $W + c$ or c is still used as the initial point. That is because when $\alpha = 1$, there are no critical point of f and g, so not to mention the trajectory of critical point; when $0 \leqslant \alpha < 1$, the critical point is ∞ and there does not exist $W + c$ or c in the trajectory of ∞, so the image iterated from $W + c$ or c is not genuine generalized M-set.

Definition 1. Assume $f(z_n) = z_n^\alpha + W + c$ $(\alpha < 0$ or $\alpha > 1)$ is a complex map importing additive noise perturbation W on the Riemann sphere $\hat{C}$, M_f denotes the collection of complex number c when the trajectory of point $W + c$ in C is bounded, i.e.

$$M_f = \big\{c \in C\colon\ \{f^k(W + c)\}_{k=1}^\infty \text{ is bounded}\big\} = \big\{c \in C\colon\ W + c, (W + c)^\alpha + W + c, \ldots \nrightarrow \infty,\ k \to \infty\big\},$$

then M_f is the generalized M-set corresponding to f.

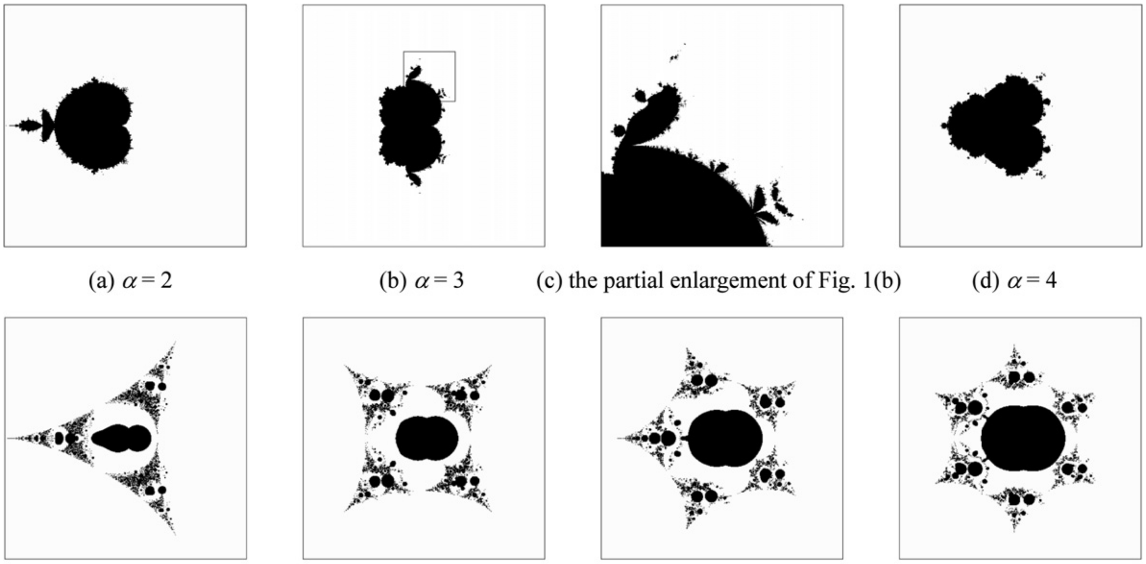

(a) $\alpha = 2$ (b) $\alpha = 3$ (c) the partial enlargement of Fig. 1(b) (d) $\alpha = 4$

(e) $\alpha = -2$ (f) $\alpha = -3$ (g) $\alpha = -4$ (h) $\alpha = -5$

Fig. 1. Dynamic additive noise perturbed generalized M-sets for integer index number.

Definition 2. Let $g(z_n) = \gamma(\lambda, k_1, k_2, \boldsymbol{w}_n) z_n^\alpha + c$ ($\alpha < 0$ or $\alpha > 1$) is a complex map importing multiplicative noise perturbation γ on the Riemann sphere $\hat{C}, M_g$ denotes the collection of complex number c when the trajectory of point c in C, i.e.

$$M_g = \left\{c \in C\colon \left\{g^k(c)\right\}_{k=1}^{\infty} \text{ is bounded}\right\} = \left\{c \in C\colon c, \gamma(\lambda, k_1, k_2, \boldsymbol{w}_n)c^\alpha + c, \ldots \nrightarrow \infty,\ k \to \infty\right\},$$

then M_g is the generalized M-set corresponding to g.

Definition 2 indicates: If $c \in M_f$, then the instant velocity of Brownian particle is bounded after the action of $W + c$, that is to say the drops into potential well; If $c \in \overline{M_f}$, then the instant velocity of Brownian particle goes to infinity after the action of $W + c$, that is to say the particle escapes out of potential well [12]. Definitions 1 and 2 are the theoretic bases of computer images using the escape-time algorithm to portray M_f and M_g [2].

2. Experiment and results

Select escape-radius as $R = 30$ and escape-time restriction as $N = 100$, the authors plot the additive noise and multiplicative noise perturbed generalized M-sets for Eqs. (5) and (8) using escape-time algorithm. Denote α as $\alpha = \pm(\eta + \varepsilon)$, where η is a positive integer and ε is a decimal, i.e. $0 < \varepsilon < 1$. When $\alpha > 0$, the black in the figure is the stable region while the white is the escape region; when $\alpha < 0$, the white in the figure is the stable region while the black is the escape region.

2.1. Additive noise perturbed generalized M-sets

In Figs. 1 and 2, the perturbed intensity coefficients are $m_1 = 0.3$ and $m_2 = 0$. When $\alpha > 0$, the stable region is embedded in the escape region and when $\alpha < 0$, the escape region is embedded in the stable region. The generalized M-set can depict the threshold of impulse received by Brownian particles that drop into or escape out of double potential well [12], so the generalized M-sets of $\alpha > 0$ in Figs. 1 and 2 visually present the upper bound of impulse $W + c$ received by Brownian particles that moved in double potential well. The perturbed generalized M-set is similar to the flower composed by $\eta - 1$ major petals when $\alpha = \eta$; when $\alpha = -\eta$, the generalized M-set is similar to the constellation structure that $\eta + 1$ secondary planet constellations circle a central planet. Enlarging partially Fig. 1(c), we find that innumerable little petal sequence that arranges according to some rule clings to the boundary of generalized M-set. This structure nestedly appears on the different levels, and the petal's distributing of the generalized M-sets embodies the topological invariance, i.e. self-similarity. The perturbed generalized M-sets for integer index number no longer have the property of rotation symmetry and the structures of their major petals or secondary planet constellations have changed a lot.

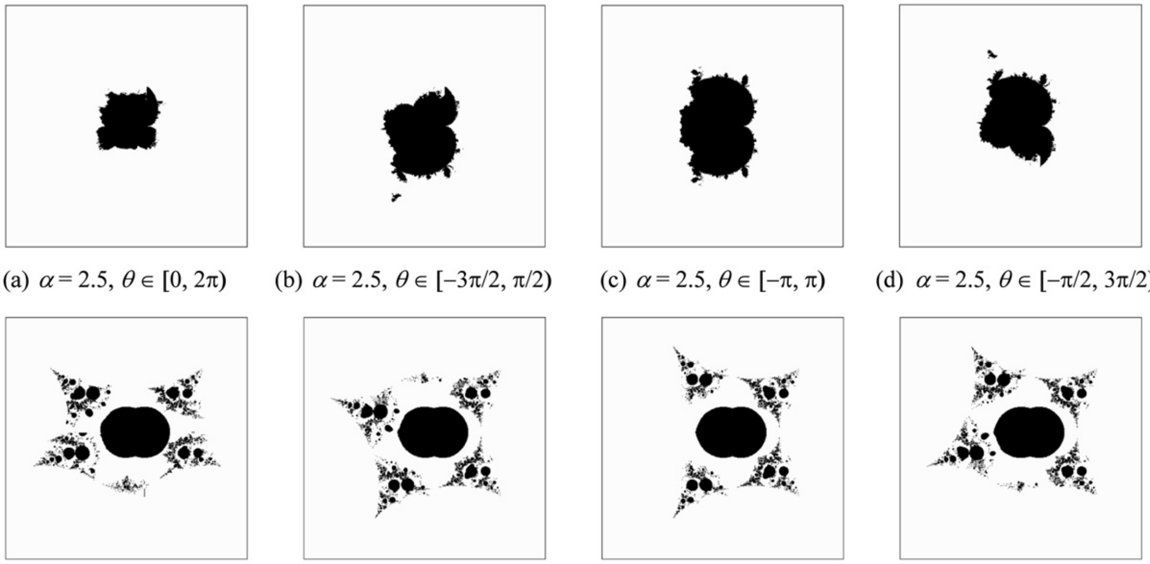

(a) $\alpha = 2.5$, $\theta \in [0, 2\pi)$ (b) $\alpha = 2.5$, $\theta \in [-3\pi/2, \pi/2)$ (c) $\alpha = 2.5$, $\theta \in [-\pi, \pi)$ (d) $\alpha = 2.5$, $\theta \in [-\pi/2, 3\pi/2)$

(e) $\alpha = -3.5$, $\theta \in [0, 2\pi)$ (f) $\alpha = -3.5$, $\theta \in [-3\pi/2, \pi/2)$ (g) $\alpha = -3.5$, $\theta \in [-\pi, \pi)$ (h) $\alpha = -3.5$, $\theta \in [-\pi/2, 3\pi/2)$

Fig. 2. Dynamic additive noise perturbed generalized M-sets for decimal index number.

Property 1. Construct generalized M-sets with integer index number for complex mapping $f(z_n) = z_n^\alpha + W + c$ ($\alpha < 0$ or $\alpha > 1$). If $m_2 = 0$, then

$$f^k(c, W) = \overline{f^k(\bar{c}, W)} \quad (k = 1, 2, \ldots, N).$$

Proof. Use the mathematical induction: For $f(c, W) = (W + c)^\alpha + W + c$, $f(\bar{c}, W) = (W + \bar{c})^\alpha + W + \bar{c}$. Since $m_2 = 0$, there is $W = \bar{W}$. So we can obtain the result as follows

$$f(c, W) = \overline{f(\bar{c}, W)}.$$

If $f^{k-1}(c, W) = \overline{f^{k-1}(\bar{c}, W)}$ is tenable, then there is

$$f^k(c, W) = f^{k-1}\big(f(c, W)\big) = f^{k-1}\big(\overline{f(\bar{c}, W)}\big) = \overline{f^{k-1}\big(f(\bar{c}, W)\big)} = \overline{f^k(\bar{c}, W)}. \qquad \square$$

The proposition is tenable. Property 1 indicates the additive noise perturbed generalized M-sets with integer index number constructed from Eq. (5) are symmetrical about *x*-axis (shown in Fig. 1). It shows that the variety rule of velocity of the Brownian particles are the same when the impulse $W + c$ and its conjugate impulse $\bar{W} + \bar{c}$ act on the particles respectively [12].

It can be seen through observing Fig. 2 that when $\alpha = \eta + \varepsilon$, the generalized M-set is similar to a flower composed by $\eta - 1$ major petals and a part one (also called embryonic petal) and the embryonic petal gradually develop into an intact one with the increase of ε; the generalized M-set when $\alpha = -(\eta + \varepsilon)$ is similar to an asymmetry constellation structure that $\eta + 1$ secondary planet constellations and a part one circle a central planet and the part one gradually develops into an intact one with the increase of ε. The structure of perturbed generalized M-sets for decimal index number have changed a lot compared with the generalized M-sets without perturbation.

The structural characteristic of generalized M-sets when $\alpha = \pm(\eta + \varepsilon)$ can be explained as follows: Construct generalized M-set from Eq. (5). For calculating z^α, use DeMoivre theory

$$z^\alpha = r^\alpha(\cos\alpha\theta + i\sin\alpha\theta). \tag{9}$$

For every iteration of Eq. (5), z always transform from rectangular coordinates to polar coordinates to calculate z^α. Then transform back into the rectangular coordinates and add perturbation W and complex constant c to itself. When transform the rectangular coordinates (x, y) of complex plane into its polar coordinates (r, θ), the range of phase angle θ generally can be selected from the following four instances: $\theta \in [0, 2\pi)$, $\theta \in [-3\pi/2, \pi/2)$, $\theta \in [-\pi, \pi)$ or $\theta \in [-\pi/2, 3\pi/2)$. When $\alpha = \pm\eta$, there is no affection on the use of Eq. (9) because of

$$\begin{cases} \cos(\alpha\theta) = \cos(\alpha\theta + 2\pi\alpha), \\ \sin(\alpha\theta) = \sin(\alpha\theta + 2\pi\alpha). \end{cases} \tag{10}$$

While $\alpha = \pm(\eta + \varepsilon)$, Eq. (10) is untenable. So the selection of the range of θ determines the evolution of generalized M-set, i.e. the dynamical characteristic of particles follows different rules. What is more, in the use of formula (10), $\alpha\theta$ may go beyond the range of above four instances: $\theta \in [0, 2\pi)$, $\theta \in [-3\pi/2, \pi/2)$, $\theta \in [-\pi, \pi)$ or $\theta \in [-\pi/2, 3\pi/2)$; hence the modulation of $\alpha\theta \pm 2m\pi$ $(m = 1, 2, \ldots)$, is needed which induced the discontinuity and collapse of generalized M-set and thereby the generation of embryonic petal. It is obvious that the embryonic petal of generalized M-set only appear when α is a decimal. In addition, the selection of phase angle θ is discontinuous in positive x-axis, positive y-axis, negative x-axis and negative y-axis which induces the embryonic petals only appearing in the four positions.

Property 2. Constructing generalized M-sets for decimal index number from complex mapping $f(z_n) = z_n^\alpha + W + c$ $(\alpha < 0$ or $\alpha > 1)$. When $\theta \in [-\pi, \pi)$ is selected as the phase angle, if $m_2 = 0$, then

$$f^k(c, W) = \overline{f^k(\bar{c}, W)} \quad (k = 1, 2, \ldots, N).$$

Proof. Use mathematical induction: Select the phase angle as $\theta \in [-\pi, \pi)$, let $c = |c|e^{i\theta}$, $\bar{c} = |c|e^{-i\theta}$. Since $m_2 = 0$, there is $W = \bar{W}$, and because $f(c, W) = (W + |c|e^{i\theta})^\alpha + W + |c|e^{i\theta}$, $f(\bar{c}, W) = (W + |c|e^{-i\theta})^\alpha + W + |c|e^{-i\theta}$. We can obtain

$$f(c, W) = \overline{f(\bar{c}, W)}.$$

Assume $f^{k-1}(c, W) = \overline{f^{k-1}(\bar{c}, W)}$ is tenable, then there is

$$f^k(c, W) = f^{k-1}\big(f(c, W)\big) = f^{k-1}\big(\overline{f(\bar{c}, W)}\big) = \overline{f^{k-1}\big(f(\bar{c}, W)\big)} = \overline{f^k(\bar{c}, W)}. \qquad \square$$

The proposition is tenable. Property 1 indicates: When $m_2 = 0$, if select the phase angle as $\theta \in [-\pi, \pi)$, the additive perturbed generalized M-sets for decimal index number constructed from Eq. (5) are symmetrical about x-axis (shown in Fig. 2(c) and (g)); the variety of velocity of particles are the same after the effect of the impulse $W + c$ and its conjugate impulse $\bar{W} + \bar{c}$.

Property 3. Construct generalized M-sets for decimal index number from complex mapping $f(z_n) = z_n^\alpha + W + c$ $(\alpha < 0$ or $\alpha > 1)$, when $\theta \in [-3\pi/2, \pi/2)$ and $\theta \in [-\pi/2, 3\pi/2)$ are selected as phase angle, if $m_2 = 0$. Then

$$f^k(c, W)\big|_{\theta \in [-3\pi/2, \pi/2)} = \overline{f^k(\bar{c}, W)}\big|_{\theta \in [-\pi/2, 3\pi/2)} \quad (k = 1, 2, \ldots, N).$$

Proof. The selections of phase angles $\theta \in [-3\pi/2, \pi/2)$ and $\theta \in [-\pi/2, 3\pi/2)$ are symmetrical about x-axis. Hence when $\theta \in [-3\pi/2, \pi/2)$ is selected, if $c = |c|e^{i\theta}|_{\theta \in [-3\pi/2, \pi/2)}$, then the conjugacy of c can be denoted as $\bar{c} = |c|e^{-i\theta}|_{\theta \in [-\pi/2, 3\pi/2)}$ when phase angle is selected as $\theta \in [-\pi/2, 3\pi/2)$. The above conclusion can be deduced by the proving process of Property 2. $\square$

Property 3 indicates: When $m_2 = 0$, turning 180° by x-axis of the perturbed generalized M-sets whose phase angle are selected as $\theta \in [-3\pi/2, \pi/2)$, the perturbed generalized M-sets whose phase angle are selected as $\theta \in [-\pi/2, 3\pi/2)$ are obtained and vice versa (shown in Fig. 2(b), (d), (f) and (h)). The variety of velocity of particles are the same when the particles are in the affection of impulse $W + c$ whose phase angle is selected as $\theta \in [-3\pi/2, \pi/2)$ and impulse $\bar{W} + \bar{c}$ whose phase angle is selected as $\theta \in [-\pi/2, 3\pi/2)$, respectively.

2.2. Multiplicative noise perturbed generalized M-sets

Figs. 3 and 4 are dynamic multiplicative noise perturbed generalized M-sets constructed by Eq. (8), whose intensity coefficients are $k_1 = 0.3$ and $k_2 = 0$, respectively. When $\alpha > 0$, the stable region is embedded in the escape region; while $\alpha < 0$, the escape region is in the stable region. Because of the disturbance of the dynamic multiplicative noise, the structure of the perturbed generalized M-sets changes a lot compared with the generalized M-sets without perturbation.

It can be seen through observing Fig. 3 that the generalized M-set when $\alpha = \eta$ is similar to a flower composed by $\eta - 1$ major petals; the generalized M-set when $\alpha = -\eta$ is similar to an asymmetry constellation structure that $\eta + 1$ secondary planet constellations circle a central planet. If η is an even number, the generalized M-sets is symmetrical about x-axis; If η is odd number, the generalized M-sets is symmetrical about x-axis and y-axis. Enlarging partially Fig. 3(c), we find that innumerable little petal sequence that arranges according to some rule clings to the boundary of generalized M-set. This structure nestedly appears on the different levels, and the petal's distributing of the generalized M-sets embodies the topological invariance, i.e. self-similarity.

Property 4. Construct generalized M-sets for integer index number from complex mapping $g(z_n) = \gamma(\lambda, k_1, k_2, \boldsymbol{w}_n) z_n^\alpha + c$ $(\alpha < 0$ or $\alpha > 1)$, when $\alpha = 2j$ $(j = 0, \pm 1, \pm 2, \ldots)$, there is

$$g^k(c, \gamma) = \overline{g^k(\bar{c}, \gamma)} \quad (k = 1, 2, \ldots, N);$$

when $\alpha = 2j + 1$ $(j = \pm 1, \pm 2, \ldots)$, there is

$$g^k(c, \gamma) = \overline{g^k(\bar{c}, \gamma)} = -\overline{g^k(-\bar{c}, \gamma)}.$$

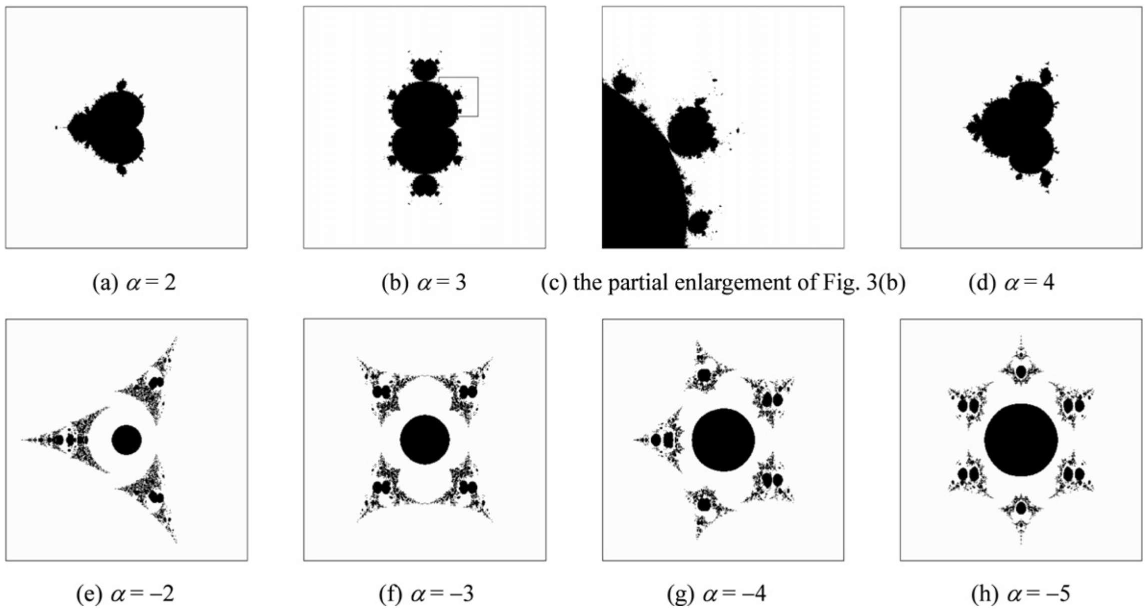

Fig. 3. Dynamic multiplicative noise perturbed generalized M-sets for integer index number.

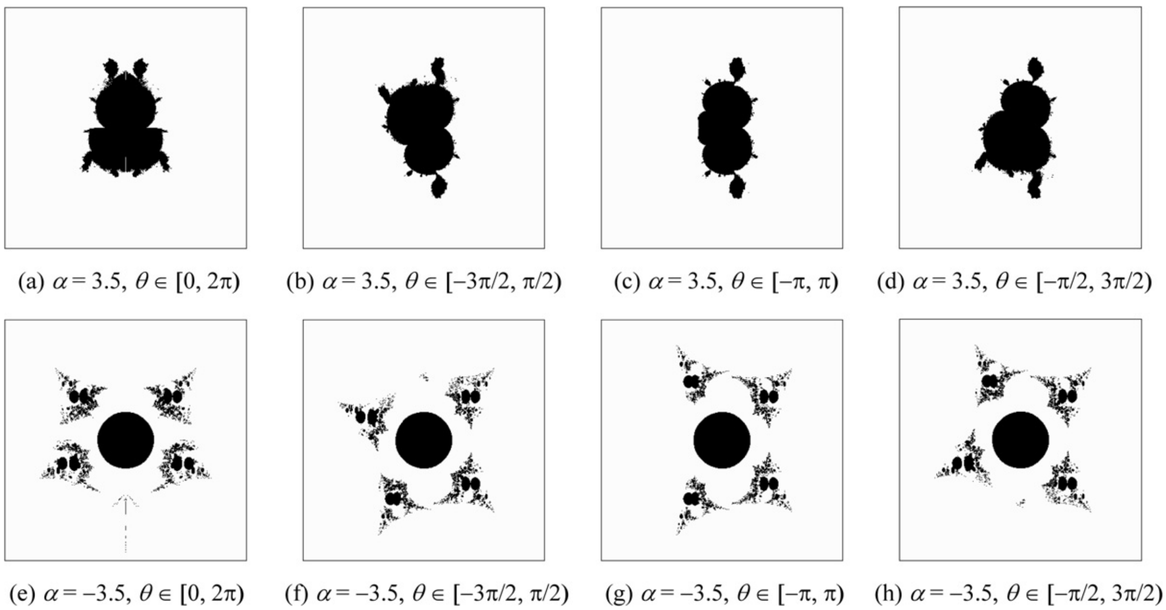

Fig. 4. Dynamic multiplicative noise perturbed generalized M-sets for decimal index number.

Proof. Using the mathematical induction, for $g^1(c,\gamma) = \gamma c^\alpha + c$, $g^1(\bar{c},\gamma) = \gamma(\bar{c})^\alpha + \bar{c}$ and $g(-\bar{c},\gamma) = \gamma(-\bar{c})^\alpha - \bar{c}$. γ is inlet perturbations of F on the x-axis and y-axis, where $\gamma_x = \lambda_1 + k_1 \boldsymbol{w}_n$, and $\gamma_y = \lambda_2 + k_2 \boldsymbol{w}_n$. So $\gamma_x = \bar{\gamma}_x$, $\gamma_y = \bar{\gamma}_y$.

If $\alpha = 2j$ $(j = 0, \pm 1, \pm 2, \ldots)$, then

$$g(c,\gamma) = \overline{g(\bar{c},\gamma)}.$$

If $\alpha = 2j+1$ $(j = \pm 1, \pm 2, \ldots)$, then

$$g(c,\gamma) = \overline{g(\bar{c},\gamma)} = -\overline{g(-\bar{c},\gamma)}.$$

If when $\alpha = 2j$, $g^{k-1}(c,\gamma) = \overline{g^{k-1}(\bar{c},\gamma)}$ is tenable and when $\alpha = 2j+1$, $g^{k-1}(c,\gamma) = \overline{g^{k-1}(\bar{c},\gamma)} = -\overline{g^{k-1}(-\bar{c},\gamma)}$ is tenable.

Then there are

$$g^k(c,\gamma) = g^{k-1}\big(g(c,\gamma)\big) = g^{k-1}\big(\overline{g(\bar{c},\gamma)}\big) = \overline{g^{k-1}\big(g(\bar{c},\gamma)\big)} = \overline{g^k(\bar{c},\gamma)},$$

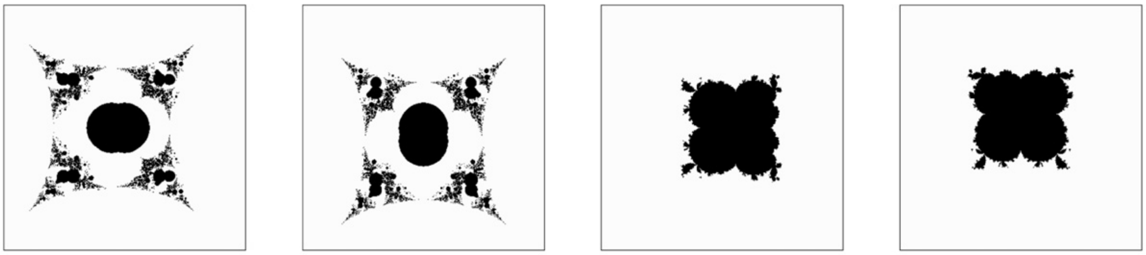

(a) $\alpha = -3$, $m_1 = 0.2$, $m_2 = 0$ (b) $\alpha = -3$, $m_1 = 0$, $m_2 = 0.2$ (c) $\alpha = 5$, $m_1 = -0.2$, $m_2 = 0$ (d) $\alpha = 5$, $m_1 = 0$, $m_2 = -0.2$

Fig. 5. Dynamic additive noise perturbed generalized M-sets with integer index for intensity coefficients m_1 and m_2.

and

$$g^k(c,\gamma) = g^{k-1}\big(g(c,\gamma)\big) = g^{k-1}\big(-\overline{g(-\bar{c},\gamma)}\big) = -\overline{g^{k-1}\big(g(-\bar{c},\gamma)\big)} = -\overline{g^k(-\bar{c},\gamma)}. \qquad \square$$

The proposition is tenable. Property 4 indicates that the multiplicative perturbed generalized M-sets for even index number constructed from Eq. (8) are symmetrical about x-axis (shown in Fig. 3(a), (d), (e) and (g)) and the generalized M-sets for odd index number are both symmetrical about x-axis and y-axis (shown in Fig. 3(b), (f) and (h)).

It can be seen through observing Fig. 4 that the generalized M-set when $\alpha = \eta + \varepsilon$ is similar to a flower composed by $\eta - 1$ major petals and a part one (also called embryonic petal) and the embryonic petal gradually develop into an intact one with the increase of ε; the generalized M-set when $\alpha = -(\eta + \varepsilon)$ is similar to an asymmetry constellation structure that $\eta + 1$ secondary planet constellations and a part one circle a central planet and the part one gradually develops into an intact one with the increase of ε. The discontinuity evolution law of generalized M-sets may be explained in detail in the author's additive perturbed generalized M-sets for decimal index number.

Property 5. Construct generalized M-sets for decimal index number from complex mapping $g(z_n) = \gamma(\lambda, k_1, k_2, \boldsymbol{w}_n) z_n^{\alpha} + c$ ($\alpha < 0$ or $\alpha > 1$). If $\theta \in [-\pi, \pi)$ is selected as phase angle, then there is

$$g^k(c,\gamma) = \overline{g^k(\bar{c},\gamma)} \quad (k = 1, 2, \ldots, N).$$

Proof. Using the mathematical induction: Selecting the phase angle as $\theta \in [-\pi, \pi)$, assume $c = |c|e^{i\theta}$ and $\bar{c} = |c|e^{-i\theta}$, $\gamma_x = \bar{\gamma}_x$ and $\gamma_y = \bar{\gamma}_y$. Because $g(c,\gamma) = \gamma c^{\alpha} + c = \gamma(|c|e^{i\theta})^{\alpha} + |c|e^{i\theta}$, $g^1(\bar{c},\gamma) = \gamma(\bar{c})^{\alpha} + \bar{c} = \gamma(|c|e^{-i\theta})^{\alpha} + |c|e^{-i\theta}$. There is

$$g(c,\gamma) = \overline{g(\bar{c},\gamma)}.$$

Assume $g^{k-1}(c,\gamma) = \overline{g^{k-1}(\bar{c},\gamma)}$, then there is

$$g^k(c,\gamma) = g^{k-1}\big(g(c,\gamma)\big) = g^{k-1}\big(\overline{g(\bar{c},\gamma)}\big) = \overline{g^{k-1}\big(f(\bar{c},\gamma)\big)} = \overline{g^k(\bar{c},\gamma)}. \qquad \square$$

The proposition is tenable. Property 5 indicates: If select the phase angle $\theta \in [-\pi, \pi)$, the multiplicative perturbed generalized M-sets for decimal index number constructed from Eq. (8) are symmetrical about x-axis (Fig. 4(c) and (g)).

Property 6. Construct generalized M-sets for decimal index number from complex mapping $g(z_n) = \gamma(\lambda, k_1, k_2, \boldsymbol{w}_n) z_n^{\alpha} + c$ ($\alpha < 0$ or $\alpha > 1$). If $\theta \in [-3\pi/2, \pi/2)$ and $\theta \in [-\pi/2, 3\pi/2)$ are selected as phase angle, then there is

$$g^k(c,\gamma)\big|_{\theta\in[-3\pi/2,\pi/2)} = \overline{g^k(\bar{c},\gamma)}\big|_{\theta\in[-\pi/2,3\pi/2)} \quad (k = 1, 2, \ldots, N).$$

Proof. The selections of the phase angles $\theta \in [-3\pi/2, \pi/2)$ and $\theta \in [-\pi/2, 3\pi/2)$ are symmetrical about x-axis. So when $\theta \in [-3\pi/2, \pi/2)$ is selected, if $c = |c|e^{i\theta}|_{\theta\in[-3\pi/2,\pi/2)}$, then the conjugacy of c can be denoted as $\bar{c} = |c|e^{-i\theta}|_{\theta\in[-\pi/2,3\pi/2)}$ when phase angle is selected as $\theta \in [-\pi/2, 3\pi/2)$. The above conclusion can be deduced by the proving process of Property 5. $\square$

Property 6 indicates: Turning 180° by x-axis of the perturbed generalized M-sets whose phase angle are selected as $\theta \in [-3\pi/2, \pi/2)$, the perturbed generalized M-sets whose phase angle are selected as $\theta \in [-\pi/2, 3\pi/2)$ are obtained and vice versa (shown in Fig. 4(b), (d), (f) and (h)).

2.3. The affection of additive perturbation to generalized M-set

Change the intensity coefficients of perturbation, the generalized M-set will change correspondingly. Figs. 5 and 6 are dynamic additive and multiplicative noise perturbed generalized M-sets with integer index for different intensity coefficients,

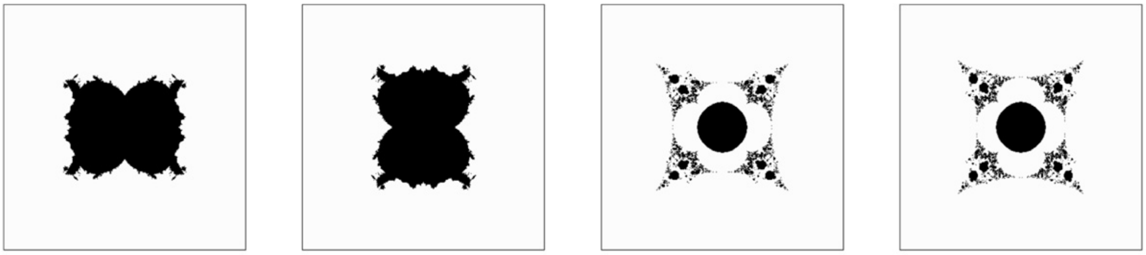

(a) $\alpha = 5$, $k_1 = -0.3$, $k_2 = 0.1$ (b) $\alpha = 5$, $k_1 = 0.1$, $k_2 = -0.3$ (c) $\alpha = -3$, $k_1 = 0.3$, $k_2 = 0.4$ (d) $\alpha = -3$, $k_1 = 0.4$, $k_2 = 0.3$

Fig. 6. Dynamic multiplicative noise perturbed generalized M-sets with integer index for intensity coefficients k_1 and k_2.

respectively. From Fig. 5 we find that when $\alpha = 5$ or -3, generalized M-sets with intensity coefficients being m_2 and m_1 may be obtain by turning generalized M-sets with intensity coefficients being m_1 and m_2 for $\pi/2$ around the origin and vice versa. From Fig. 6, when $\alpha = 5$ or -3, generalized M-sets with intensity coefficients being k_2 and k_1 may be obtain by turning generalized M-sets with intensity coefficients being k_1 and k_2 for $\pi/2$ around the origin and vice versa.

Property 7. Construct generalized M-set for integer index number from complex mapping $f(z_n) = z_n^\alpha + W + c$ ($\alpha < 0$ or $\alpha > 1$), when $\alpha = 4j + 1$ ($j = \pm 1, \pm 2, \ldots$), there is

$$f^k\left(ce^{i\frac{\pi}{2}(4m+1)}, We^{i\frac{\pi}{2}(4m+1)}\right) = e^{i\frac{\pi}{2}(4m+1)} f^k(c, W) \quad (m = 0, \pm 1, \pm 2, \ldots;\ k = 1, 2, \ldots, N).$$

Proof. Using the mathematical induction, when $\alpha = 4j + 1$ ($j = \pm 1, \pm 2, \ldots$), there is

$$\begin{aligned} f\left(ce^{i\frac{\pi}{2}(4m+1)}, We^{i\frac{\pi}{2}(4m+1)}\right) &= \left(We^{i\frac{\pi}{2}(4m+1)} + ce^{i\frac{\pi}{2}(4m+1)}\right)^\alpha + We^{i\frac{\pi}{2}(4m+1)} + ce^{i\frac{\pi}{2}(4m+1)} \\ &= e^{i\frac{\pi}{2}(4m+1)}\left[(W + c)^\alpha + W + c\right], \end{aligned}$$

i.e.

$$f\left(ce^{i\frac{\pi}{2}(4m+1)}, We^{i\frac{\pi}{2}(4m+1)}\right) = e^{i\frac{\pi}{2}(4m+1)} f(c, W).$$

If $f^{k-1}(ce^{i\frac{\pi}{2}(4m+1)}, We^{i\frac{\pi}{2}(4m+1)}) = e^{i\frac{\pi}{2}(4m+1)} f^{k-1}(c, W)$, then

$$\begin{aligned} f^k\left(ce^{i\frac{\pi}{2}(4m+1)}, We^{i\frac{\pi}{2}(4m+1)}\right) &= f^{k-1}\left[f\left(ce^{i\frac{\pi}{2}(4m+1)}, W^{i\frac{\pi}{2}(4m+1)}\right)\right] = f^{k-1}\left[e^{i\frac{\pi}{2}(4m+1)} f(c, W)\right] \\ &= e^{i\frac{\pi}{2}(4m+1)} f^{k-1}\left[f(c, W)\right] = e^{i\frac{\pi}{2}(4m+1)} f^k(c, W). \qquad \square \end{aligned}$$

The proposition is tenable. Property 7 indicates: When $\alpha = 4j + 1$, the generalized M-sets with intensity coefficients being m_2 and m_1 can be obtained from turning the generalized M-sets with intensity coefficients being m_1 and m_2 for $\pi(4m + 1)/2$ around the origin and vice versa (shown in Fig. 5(a)–(d)). Property 7 also indicates: The variety of velocity of the particles of the impulse $W + c$ firstly turning for $\pi(4m + 1)/2$ and then acting on the particles equals to that of the impulse $W + c$ firstly acting on the particles and then turning for $\pi(4m + 1)/2$.

If inlet perturbations of F on the x-axis and y-axis are complex number c and γ, there are $\gamma_x = \lambda_1 + k_1\boldsymbol{w}_n$, and $\gamma_y = \lambda_2 + k_2\boldsymbol{w}_n$, then for complex number $ce^{i\frac{\pi}{2}(4m+1)}$ ($m = 0, \pm 1, \pm 2, \ldots$), $\tilde{\gamma}$ is inlet perturbations of F on the x-axis and y-axis, where $\tilde{\gamma}_x = \lambda_2 + k_2\boldsymbol{w}_n$, and $\tilde{\gamma}_y = \lambda_1 + k_1\boldsymbol{w}_n$.

Property 8. Construct generalized M-sets for integer index number from complex mapping $g(z_n) = \gamma(\lambda, k_1, k_2, \boldsymbol{w}_n)z_n^\alpha + c$ ($\alpha < 0$ or $\alpha > 1$), when $\alpha = 4j + 1$ ($j = \pm 1, \pm 2, \ldots$), there is

$$g^k\left(ce^{i\frac{\pi}{2}(4m+1)}, \tilde{\gamma}\right) = e^{i\frac{\pi}{2}(4m+1)} g^k(c, \gamma) \quad (m = 0, \pm 1, \pm 2, \ldots;\ k = 1, 2, \ldots, N).$$

Proof. Use the mathematical induction: When $\alpha = 4j + 1$ ($j = \pm 1, \pm 2, \ldots$), there is

$$g\left(ce^{i\frac{\pi}{2}(4m+1)}, \tilde{\gamma}\right) = \tilde{\gamma}\left(ce^{i\frac{\pi}{2}(4m+1)}\right)^\alpha + ce^{i\frac{\pi}{2}(4m+1)} = e^{i\frac{\pi}{2}(4m+1)}\left(\gamma c^\alpha + c\right),$$

i.e.

$$g\left(ce^{i\frac{\pi}{2}(4m+1)}, \tilde{\gamma}\right) = e^{i\frac{\pi}{2}(4m+1)} g(c, \gamma).$$

If $g^{k-1}(ce^{i\frac{\pi}{2}(4m+1)}, \tilde{\gamma}) = e^{i\frac{\pi}{2}(4m+1)} g^{k-1}(c, \gamma)$, then

$$\begin{aligned} g^k\left(ce^{i\frac{\pi}{2}(4m+1)}, \tilde{\gamma}\right) &= g^{k-1}\left[g\left(ce^{i\frac{\pi}{2}(4m+1)}, \tilde{\gamma}\right)\right] = g^{k-1}\left[e^{i\frac{\pi}{2}(4m+1)} g(c, \gamma)\right] = e^{i\frac{\pi}{2}(4m+1)} g^{k-1}\left[g(c, \gamma)\right] \\ &= e^{i\frac{\pi}{2}(4m+1)} g^k(c, \gamma). \qquad \square \end{aligned}$$

The proposition is tenable. Property 8 indicates: When $\alpha = 4j + 1$, the generalized M-set with intensity coefficients being k_2 and k_1 can be obtained from turning the generalized M-set with intensity coefficients being k_1 and k_2 for $\pi(4m+1)/2$ around the origin and vice versa (shown in Fig. 6(a)–(d)).

3. Conclusions

(1) Adopting the experimental mathematics method combining complex variable function and computer aided drawing, this paper constructed a series of additive and multiplicative perturbed generalized M-sets, studied the structural characteristics and fission-evolution law of the generalized M-sets, and discussed influence of stochastic perturbed parameters to the structure of generalized M-sets. On the basis of this, describe vividly the complex Brownian movement law using the fractal structure of additive noise generalized M-sets.

(2) The generalized M-sets have boundlessly complex structures, which cannot be described by Euclidean space. In some sense, they have boundless information in depth or extent just like the vast universe that our solar system exists in. Describing the complex Brownian movement using the fractal structure of generalized M-sets is edificatory to people studying problems in their respective professional fields or some interdisciplinary fields.

References

[1] H.O. Peitgen, D. Saupe, The Science of Fractal Images, Springer-Verlag, Berlin, 1988, pp. 137–218.
[2] X.Y. Wang, The Fractal Mechanism of Generalized M–J Set, Dalian University of Technology Press, Dalian, 2002, pp. 1–58.
[3] U.G. Gujar, V.C. Bhavsar, Fractals from $z \leftarrow z^\alpha + c$ in the complex c-plane, Computers & Graphics 15 (3) (1991) 441–449.
[4] E.F. Glynn, The evolution of the Gingerbread Man, Computers & Graphics 15 (4) (1991) 579–582.
[5] X.Y. Wang, X.D. Liu, W.Y. Zhu, et al., Analysis of c-plane fractal images from $z \leftarrow z^\alpha + c$ for $\alpha < 0$, Fractals 8 (3) (2000) 307–314.
[6] J.C. Sasmor, Fractals for functions with rational exponent, Computers & Graphics 28 (4) (2004) 601–615.
[7] M. Romera, G. Pastor, G. Álvarez, et al., External arguments of Douady cauliflowers in the Mandelbrot set, Computers & Graphics 28 (3) (2004) 437–449.
[8] G. Pastor, M. Romera, G. Álvarez, et al., Chaotic bands in the Mandelbrot set, Computers & Graphics 28 (5) (2004) 779–784.
[9] Y.H. Geum, Y.I. Kim, Accurate computation of component centers in the degree-n bifurcation set, Comput. Math. Appl. 48 (1–2) (2004) 163–175.
[10] X.Y. Wang, P.J. Chang, Research on fractal structure of generalized M–J sets utilized Lyapunov exponents and periodic scanning techniques, Appl. Math. Comput. 175 (2) (2006) 1007–1025.
[11] C. Beck, Physical meaning for Mandelbrot and Julia sets, Phys. D 125 (1999) 171–182.
[12] X.Y. Wang, Q.Y. Meng, Research on physical meaning for the generalized Mandelbrot–Julia sets based on Langevin problem, Acta Phys. Sinica 53 (2) (2004) 388–395.
[13] J. Argyris, I. Andreadis, G. Pavlos, et al., On the influence of noise on the correlation dimension of chaotic attractors, Chaos Solitons Fractals 9 (3) (1998) 343–361.
[14] A. Lasota, M.C. Makey, Chaos, Fractals and Noise: Stochastic Aspects of Dynamical Systems, Springer-Verlag, New York, 1994, pp. 69–106.
[15] T. Kapitaniak, Experimental synchronization of chaos using continuous control, Internat. J. Bifur. Chaos 4 (2) (1994) 483–488.
[16] J. Argyris, I. Andreadis, T.E. Karakasidis, On perturbations of the Mandelbrot map, Chaos Solitons Fractals 11 (7) (2000) 1131–1136.
[17] J. Argyris, T.E. Karakasidis, I. Andreadis, On the Julia set of the perturbed Mandelbrot map, Chaos Solitons Fractals 11 (13) (2000) 2067–2073.
[18] J. Argyris, T.E. Karakasidis, I. Andreadis, On the Julia set of a noise-perturbed Mandelbrot map, Chaos Solitons Fractals 13 (2) (2002) 245–252.
[19] P. L'Ecuyer, Efficient and portable combined random number generators, Comm. ACM 31 (6) (1988) 742–749, and 774.
[20] W.H. Press, S.A. Teukolsky, Portable random number generators, Comput. Phys. 6 (1992) 522–524.
[21] M. Klein, Mandelbrot set in a non-analytic map, Z. Naturforsch. A 43 (1988) 819–820.